Catalyst Screening

DOI: 10.1002/anie.200701326

High-Throughput Screening of Catalysts by Combining Reaction and Analysis**

Oliver Trapp, Sven K. Weber, Sabrina Bauch, and Werner Hofstadt*

Dedicated to Süd-Chemie on the occasion of its 150th anniversary

Discovering new catalysts is crucial to the development of sustainable chemical processes for industrial applications as well as for broadening the spectrum of synthetic methodologies and techniques in chemistry. The prerequisite for the directed design of catalysts is understanding how the kinetics, in other words, the activation barrier, in the mechanism of catalysis is controlled by the structural parameters.[1] To identify rate-determining elementary steps and to develop models, comprehensive experimental kinetic data of a broad variety of substrates are necessary. Microfluidic devices integrating chemical synthesis and analysis on the same chip[2–5] are one promising approach for parallelized high-throughput (ht) kinetic measurements of catalysts with minute material consumption.[6] A unique technique for studying configurational changes in chiral compounds is dynamic chromatography[7] combining molecular interconversion and analysis under precisely controlled conditions. Recently, we reported[8] a unified equation to directly access reaction rate constants of first-order reactions of such experiments. However, commonly used (micro)reactors, in which the reaction, separation, and quantification of conversion are performed consecutively, are limited to the study of single reactions, because competing reactions lead to undefinable reaction kinetics. Here we show for the hydrogenation over highly active Pd nanoparticles and the ring-closing metathesis over the Grubbs second generation catalyst that the synchronous combination of catalysis and separation makes it possible to efficiently perform ht reaction rate measurements (147 reactions per hour) of substrate libraries. The catalytic systems for these multiphase reactions (gas–liquid–solid) were prepared by embedding the catalysts in polysiloxanes, which serve as both solvent and selective stationary separation phase. Furthermore this system can be used for cascade reactions or for preparative synthesis to produce the target compounds.

Typically, multiphase catalytic systems, which play a predominant role in industrial processes, are difficult to investigate because the interaction of the substrate with the catalyst is controlled by the mass transfer between the different phases, and therefore the apparent reaction rate is composed of the inherent reaction rate and diffusion rates. To reduce this effect, the interfacial area must be increased. Microstructured reaction systems intrinsically have a high specific interfacial area per volume, only dependent on the radius of the reaction channels; that is, for capillaries with inner diameters between 250 and 100 μm the specific interfacial area per volume ranges from 16000 to 40000 $m^2 m^{-3}$. Microfluidic systems are currently revolutionizing chemical synthesis,[9–13] because physical processes can be more easily controlled, low operation volumes minimize reagent consumption, and detection is integrated.[14] However, there are still many challenges,[15] for example, the control of mixing, because diffusion rates contribute to the apparent reaction rates, incompatibility with standard analytical instruments, and interfacing with a mass spectrometer, to mention only a few.

Our strategy unites synthesis and analysis by combining catalytic activity and separation selectivity in the polymeric stationary phase of a chromatographic separation capillary. This concept makes it possible to control the selectivity and contact time of the analytes with the catalyst. Whereas reactions during chromatographic separations were often considered to be serendipitous[16–18] or interfering side effects, appearing as overlapping peak profiles with plateau formations,[19,20] we have used this information to investigate the reaction kinetics of a broad variety of substrates.

To put this strategy into practice we focused on hydrogenations over Pd nanoparticles embedded in an inert polydimethylsiloxane matrix without any interfering protecting shell (for example, tetraalkylammonium salts as surfactants).[21] We prepared a methylvinylsiloxane–dimethylsiloxane copolymer (4.5% $Si(O)(CH_3)(CH{=}CH_2)$ groups) to coordinate Pd ions to the vinyl groups. Hydridomethylsiloxane–dimethylsiloxane copolymer (25.7% $Si(O)(CH_3)H$ groups) was added to this mixture to reduce Pd^{2+} to Pd^0 and to crosslink with the other copolymer in a Pd-catalyzed hydrosilylation reaction to form a stabilizing matrix (Figure 1).

^1H NMR measurements confirmed that the proportion of $Si(O)(CH_3)H$ groups decreased to 2.6% (starting from 16.1% in the mixture of the two polymers). The Pd nanoparticles

[*] Dr. O. Trapp, S. K. Weber, S. Bauch, W. Hofstadt
Department of Heterogeneous Catalysis
Max-Planck-Institut für Kohlenforschung
Kaiser-Wilhelm-Platz 1, 45470 Mülheim an der Ruhr (Germany)
Fax: (+49) 208-306-2995
E-mail: trapp@mpi-muelheim.mpg.de
Homepage: http://www.mpi-muelheim.mpg.de/kofo/institut/arbeitsbereiche/trapp/trapp_e.html

[**] Generous financial support by the MPI für Kohlenforschung, the DFG (Emmy Noether program (TR 542/3), and the Cusanuswerk (fellowship to S.K.W.) is gratefully acknowledged. We thank H. J. Bongard, A. Dreier, B. Spliethoff, and Dr. B. Tesche for TEM, SEM, and EDX measurements.

Supporting information for this article is available on the WWW under http://www.angewandte.org or from the author.

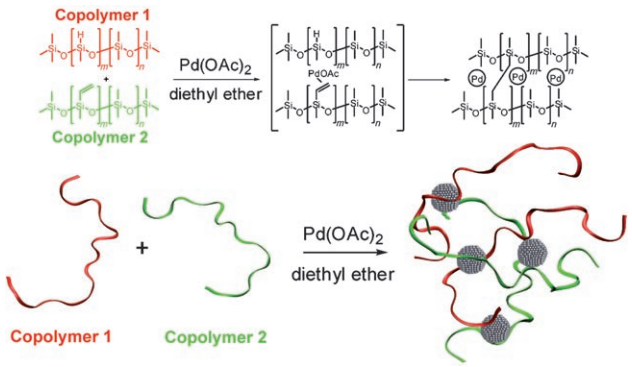

Figure 1. Preparation of highly active Pd nanoparticles embedded in a polysiloxane matrix.

were spherical and crystalline with a narrow size distribution of 3.2 nm ± 0.7 nm (determined by TEM; see the Supporting Information). Surprisingly, we observed that the morphology of the Pd nanoparticles strongly depends on the ratio of the two polysiloxanes. TEM characterization revealed that treatment with hydrogen at elevated temperatures (180–200 °C) led to larger amorphous nanoparticles (3.6 ± 1.6 nm; see the Supporting Information). The resulting viscous brownish gray polymers were then applied as a thin film onto the inner surface of fused-silica capillaries and heated to 180 °C at a rate of 0.5 K min^{-1} under hydrogen flow to provide a permanently bonded polymer. The SEM image of the capillary and the SEM and EDX patterning of Si and Pd show the fused-silica microcapillary with the Pd/polysiloxane surface coating (Figure 2). The Pd loading was extremely low, only 0.73×10^{-12} mol per cm of capillary (corresponding to approximately 27 billion Pd nanoparticles per cm with 1600 to 1700 Pd atoms per particle).

On-column catalysis was performed by coupling this Pd nanoparticle microcapillary between a pre-separation capillary (1 m) and a separation column (25 m). The purpose of the pre-separation column is to thermally equilibrate the reactants and to spatially separate the substrates of the injected compound library, which enables ht kinetic investigations because of the absence of competing reactions. Hydrogen gas was used as the reactive carrier gas. Substrates and products were quantified by flame ionization detection (FID) and identified by MS. Substrate libraries consisting of 22 unsaturated compounds (alkenes, alkynes, aromatic hydrocarbons) and functionalized compounds (nitro compounds, aldehydes, ketones) to investigate the chemoselectivity were simultaneously injected onto this column configuration at different temperatures and gas flows to vary the reaction time and to obtain temperature-dependent kinetic data. We observed extraordinary fast hydrogenations leading to complete conversion of the substrates even for Pd nanoparticle capillaries only 5 cm in length and at low reaction temperatures (60 °C). Therefore, to achieve incomplete conversions for the kinetic measurements all experiments were performed with a 2-cm-long capillary (Figure 2, Table 1) and with reaction times between 20 ms and 1 s. For some compounds, for example, *trans*-cinnamaldehyde, methylbicyclo[2.2.1]hept-5-ene-2-carboxylate, dimethylacetylenedicarboxylate, and styrene, we obtained 100 % conversion for Pd nanoparticles with the highest activity even under these mild conditions.

From temperature- and flow-dependent conversion measurements for each compound we obtained data sets which were put into kinetic models based on a Langmuir–Hinshelwood mechanism[22] to determine reaction rate constants k and activation parameters (Gibbs activation energy $\Delta G^{\neq}$, activation enthalpy $\Delta H^{\neq}$, and activation entropy $\Delta S^{\neq}$). We achieved a very good agreement when we applied first-order reaction kinetics with respect to the substrates.

The high activity of the Pd nanoparticles was corroborated by the activation parameters, which show low activation enthalpies $\Delta H^{\neq}$ and negative activation entropies $\Delta S^{\neq}$, corresponding to a restraint transition state. It is important to note that our experimental setup has the advantage of precise temperature control and that diffusion processes can be quantified and experimentally controlled by the polysiloxane used. Because we could inject simultaneously large substrate libraries (22 different substrates, see the Supporting Information), we achieved experimentally a throughput of 5880 reactions in 40 h. This corresponds to the determination of a complete set of activation parameters (see the Supporting Information) in less than 2 h. This efficiency allowed us to screen 40 systematically varied Pd nanoparticle samples and to correlate the activation energy $\Delta G^{\neq}$ with the structure of the particles. The highest activity was observed for amor-

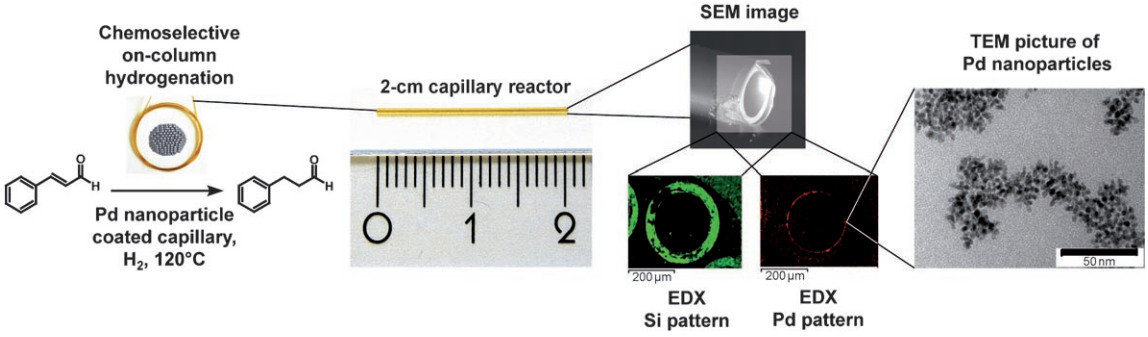

Figure 2. On-column hydrogenation over highly active Pd nanoparticles. Capillaries only 2 cm long coated with Pd nanoparticles stabilized in a polysiloxane matrix were used as the reactor. SEM and Si/Pd EDX (16 h) measurements show the coating of the fused silica microcapillaries (i.d. 250 µm, film thickness 0.25 µm).

Table 1: Selected results of the on-column hydrogenations over highly active Pd nanoparticles.

Substrate	Product	k[a] [s^{-1}]	$\Delta G^{\neq}$[b] [kJ mol^{-1}]	$\Delta H^{\neq}$ [kJ mol^{-1}]	$\Delta S^{\neq}$ [J K^{-1} mol^{-1}]	r[c] (*s.d.*)
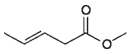	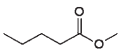	194	67.8	30.1 ±0.5	−126 ±3	0.997 (0.057)
		42	70.4	25.2 ±0.5	−152 ±4	0.996 (0.052)
		36	71.4	27.2 ±0.7	−148 ±6	0.996 (0.046)
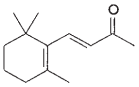	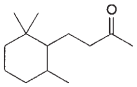	4	82.3	56.0 ±1.0	−94 ±2	0.998 (0.020)
		44	73.4	37.5 ±0.6	−121 ±3	0.999 (0.025)
		23	75.3	38.3 ±1.5	−124 ±7	0.985 (0.116)

[a] Reaction rate constant at 120 °C. [b] Gibbs activation energy $\Delta G^{\neq}$ at 25 °C. [c] Correlation factor r and residual standard deviation of the linear regression of the Eyring plot.

phous nanoparticles stabilized by a highly crosslinked polysiloxane made from a stoichiometric mixture of the two polymers. By continuous injection of a single substrate, for example, cyclohex-2-enone, onto these columns we could also preparatively hydrogenate in amounts of about 20 mg h^{-1} (see the Supporting Information).

To demonstrate the generality of our approach and the broad range of reaction kinetics that can be investigated, we focused on ring-closing metathesis[23,24] (RCM) catalyzed by the Grubbs 2nd generation catalyst. For the preparation of the catalytically active microcolumns we dissolved the Grubbs 2nd generation catalyst in dimethylpolysiloxane (GE SE 30) and coated microcapillaries (10 m) with a film thickness of 1 μm under strict exclusion of oxygen. The catalyst loading was only 1.6 μg (1.9×10^{-9} mol) per meter of capillary. The on-column catalysis was performed by coupling this column with a pre-separation column 1 m in length. Helium was used as the inert carrier gas. Eluted compounds were quantified and identified by FID and MS detection (Figure 3).

We injected a substrate library of 12 different compounds simultaneously for ring-closing metathesis onto the catalytically active separation column. In these experiments we obtained elution profiles characterized by a plateau formation between the substrate and product (see Figure 3 and the Supporting Information). These elution profiles were analyzed by the unified equation[8] (see the Supporting Information) to obtain reaction rate constants (Table 2). The dissociation and chromatographic removal of the tricyclohexylphosphine ligand (PCy_3) could not be detected; this can be explained by the fact that the phosphine ligand dissolves in the polysiloxane and can stabilize the complex after the reaction.[25] It is remarkable that the catalyst was stable over a wide temperature range (up to 150 °C) without any detectable degradation of the catalytic activity or leaching.

Activation parameters were obtained from temperature-dependent measurements: for example, for *N*,*N*-diallyltrifluoroacetamide $\Delta G^{\neq}(298\ \mathrm{K}) = 84.1\ \mathrm{kJ\,mol^{-1}}$, $\Delta H^{\neq} = (15.5 \pm 0.9)\ \mathrm{kJ\,mol^{-1}}$, $\Delta S^{\neq} = (-230 \pm 8)\ \mathrm{J\,K^{-1}\,mol^{-1}}$. These parameters corroborate recently reported theoretical calculations[26] performed in an effort to explain the high activity of the Grubbs 2nd generation catalyst. Also in these experiments by the simultaneous injection of an substrate library we achieved an extraordinary high throughput in the determination of reaction rate constants (36 rate constants per hour). The polarity of the dimethylpolysiloxane used here corresponds to a nonpolar solvent. Tuning the polarity of stationary phases with functional groups should make it possible to investigate solvent effects in continuous polarity steps.

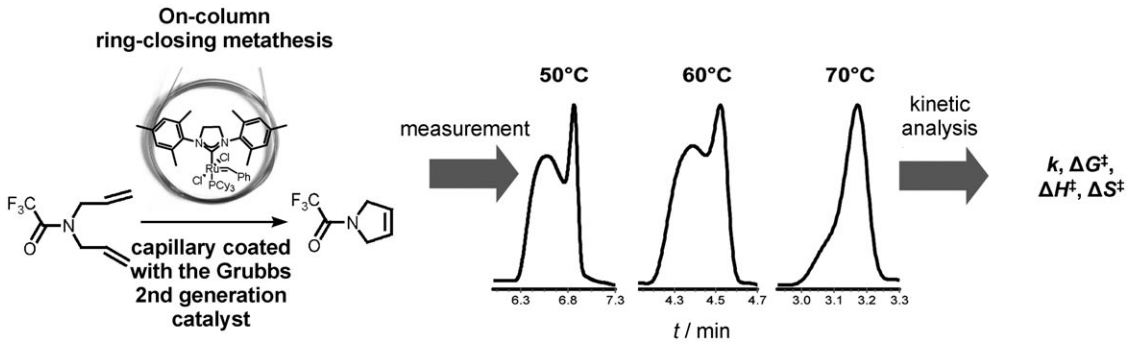

Figure 3. On-column metathesis over the Grubbs 2nd generation catalyst. In these experiments catalytic activity and separation selectivity is combined in a single 10-m-long capillary by dissolving the catalyst in the stationary separation phase. The elution profiles obtained were characterized by a pronounced conversion profile from the subsrate to the product. Kinetic analysis was performed directly with the unified equation from Ref. [8].

Table 2: Selected results of the on-column ring-closing metathesis.

Substrate	Product	T [°C]	C[a] [%]	k[b] [10^{-3} s^{-1}]	$\Delta G^{\neq}$ [kJ mol^{-1}]
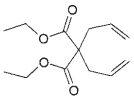	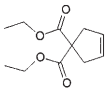	110.0	39.0	2.2	114.1
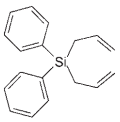	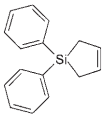	150.0	97.3	3.4	124.9
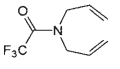	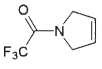	50.0	62.5	8.6	89.8
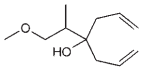	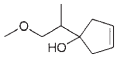	120.0	59.5	7.7	113.1
		90.0	51.0	4.9	105.6

[a] Conversion C. [b] Reaction rate constant k. Conditions: 10-m-long microcapillary (i.d. 250 μm, film thickness 1 μm), He as the inert carrier gas.

Because these catalytically active separation capillaries are easy to prepare and handle we used them in a modular design for two-step cascade reactions. We coupled a 80-cm-long column, coated with the dissolved Grubbs 2nd generation catalyst, and a 10-cm-long Pd nanoparticle column, followed by a separation column for product analysis (cf. Figure 4). We used hydrogen as a carrier gas, but the experiment could also be performed with helium in the first column section and adding hydrogen in the second section. We demonstrated that the metathesis of *N*,*N*-diallyltrifluoroacetamide followed by on-column hydrogenation is possible in less than 6 min with an overall yield of 49% (see Figure 4 and the Supporting Information).

The strategies outlined here can be generally applied to other catalytic processes, and we found that they can be utilized in the comprehensive kinetic characterization of catalysts and materials. Furthermore it can be envisioned that catalytic capillaries could be useful for selective transformations in analytical applications and for structure elucidation. Moreover, for a preparative scale-up only a stack of reactor capillaries is necessary to increase the productivity. In this approach the advantage of heterogeneous catalysis—the ready separation of catalyst and reaction product, which is normally a problem for nanopartical and homogeneous catalysts—is also conserved.

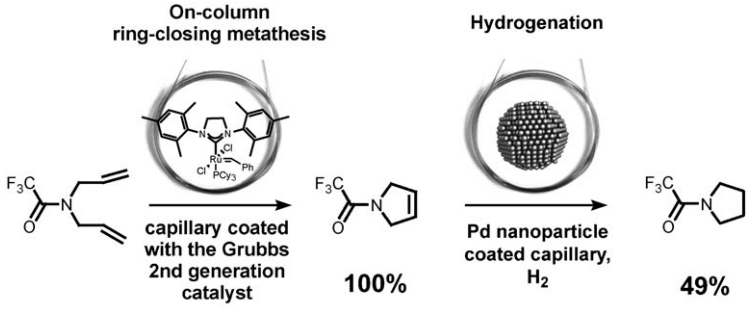

Figure 4. Modular design for a two-step on-column cascade reaction. *N*-trifluoroacetylpyrrolidine was synthesized within 6 min by coupling a 80 cm long metathesis column and a 10 cm long Pd nanoparticle hydrogenation column. H_2 was used as the reactive carrier gas.

These results impressively illustrate the (r)evolution of the chemist's toolkit from flasks and beakers to miniaturized reactors with highly selective catalysts and inherently combined separation techniques. These reactors mimic biological systems in which reactions take place efficiently at miniaturized interfaces in continuous-flow reactors. Therefore, the development of chemical microplants for the production of fine chemicals can be envisaged as a natural step in terms of energy efficiency and environmental impact.

Received: March 26, 2007
Revised: May 21, 2007
Published online: July 31, 2007

Keywords: homogeneous catalysis · hydrogenation · metathesis · multiphase reactions · nanoparticles

[1] C. T. Campbell, *Nature* **2004**, *432*, 282–283.
[2] J. Knight, *Nature* **2002**, *418*, 474–475.
[3] D. Janasek, J. Franzke, A. Manz, *Nature* **2006**, *442*, 374–380.
[4] D. Belder, M. Ludwig, L.-W. Wang, M. T. Reetz, *Angew. Chem.* **2006**, *118*, 2523–2526; *Angew. Chem. Int. Ed.* **2006**, *45*, 2463–2466.
[5] S. J. Haswell, *Nature* **2006**, *441*, 705.
[6] S. J. Haswell, P. Watts, *Green Chem.* **2003**, *5*, 240–249.
[7] O. Trapp, G. Schoetz, V. Schurig, *Chirality* **2001**, *13*, 403–414.
[8] O. Trapp, *Anal. Chem.* **2006**, *78*, 189–198.
[9] C. de Bellefon, N. Tanchoux, S. Caravieilhes, P. Grenouillet, V. Hessel, *Angew. Chem.* **2000**, *112*, 3584–3587; *Angew. Chem. Int. Ed.* **2000**, *39*, 3442–3445.
[10] J. Kobayashi, Y. Mori, K. Okamoto, R. Akiyama, M. Ueno, T. Kitamori, S. Kobayashi, *Science* **2004**, *304*, 1305–1308.
[11] P. Watts, S. J. Haswell, *Chem. Soc. Rev.* **2005**, *34*, 235–246.
[12] Y. Uozumi, Y. M. A. Yamada, T. Beppu, N. Fukuyama, M. Ueno, T. Kitamori, *J. Am. Chem. Soc.* **2006**, *128*, 15994–15995.
[13] *Micro Instrumentation* (Eds.: M. V. Koch, K. M. Van den Bussche, R. W. Chrisman), Wiley-VCH, Weinheim, **2007**.
[14] A. J. deMello, *Nature* **2006**, *442*, 394–402.
[15] G. M. Whitesides, *Nature* **2006**, *442*, 368–373.
[16] E. Gil-Av, Y. Herzberg-Minzly, *Chem. Commun.* **1961**, 316.
[17] R. Thede, E. Below, D. Haberland, S. H. Langer, *Chromatographia* **1997**, *45*, 149–154.
[18] N. A. Katsanos, R. Thede, F. Roubani-Kalantzopoulou, *J. Chromatogr. A* **1998**, *795*, 133–184.
[19] T. D. Vu, A. Seidel-Morgenstern, S. Grüner, A. Kienle, *Ind. Eng. Chem. Res.* **2005**, *44*, 9565–9574.
[20] D. W. Bassett, H. W. Habgood, *J. Phys. Chem.* **1960**, *64*, 769–773.
[21] M. T. Reetz, W. Helbig, S. A. Quaiser, U. Stimming, N. Breuer, R. Vogel, *Science* **1995**, *267*, 367–369.
[22] A. Schmidt, R. Schomäcker, *Ind. Eng. Chem. Res.* **2007**, *46*, 1677–1681.
[23] R. H. Grubbs, *Angew. Chem.* **2006**, *118*, 3845–3850; *Angew. Chem. Int. Ed.* **2006**, *45*, 3760–3765.
[24] A. Fürstner, *Angew. Chem.* **2000**, *112*, 3140–3172; *Angew. Chem. Int. Ed.* **2000**, *39*, 3012–3043.
[25] M. S. Sanford, J. A. Love, R. H. Grubbs, *J. Am. Chem. Soc.* **2001**, *123*, 6543–6554.
[26] B. F. Straub, *Angew. Chem.* **2005**, *117*, 6129–6132; *Angew. Chem. Int. Ed.* **2005**, *44*, 5974–5978.

